

Post-Blackout Response of Backup Power Supply on the Safety of Nuclear Fuel Storage Vault

Vivek K. Mishra^{1,2}, Saroj K. Panda¹, Biswanath Sen¹, M. P. Maiya³, B. P. C. Rao²

¹ Indira Gandhi Centre for Atomic Research,
Kalpakkam-603102, Tamil Nadu, India

² Homi Bhabha National Institute,
Anushaktinagar, Mumbai-400094, India

³ Department of Mechanical Engineering,
IIT Madras, Chennai-600036, India

vivekkm@igcar.gov.in; sarojdeep@gmail.com; biswa@igcar.gov.in; mpmaiya@iitm.ac.in; bpcrao.igc@nic.in

Abstract—Thermal analysis of nuclear fuel storage vault post-blackout scenario and the response from different backup power supply systems have been carried out numerically. The thermal aspects of the blackout scenario with backup power supply and its effect on the rise in temperature of the blanket and fuel containers and their enclosures are presented. The airflow inside the vault is analyzed using predicted data from the simulations. The safety of the vault was analyzed in terms of inside air temperature distributions and the temperature rise of fuels after the failure of suction blowers. The reduction in air circulation resulted in the rise in the temperature of fuels and concrete walls of the vault. The temperatures of the fuel subassemblies and magazines increase immediately after the failure of suction blowers and rise in temperature of cooling air. The repeated failure of blowers led to a fluctuation in average fuel temperature. The present study will help identify different safety measures of nuclear fuel storage systems.

Keywords: Nuclear storage, Heat transfer, Temperature distribution, Computational Fluid Dynamics (CFD), Turbulent flow.

1. Introduction

The fresh nuclear fuel before loading into the reactors is stored inside a concrete storage vault to prevent the release of radioactive particles in the vicinity of the facility. The decay of radioactive fissile materials inside the subassemblies and magazines results in heat generation that increases the temperature inside the storage vault. The subassemblies and magazines stored inside a reinforced cement concrete (RCC) dry storage vault are cooled by induced air at high velocity. The negative suction pressure at the outlets that are responsible for the flow of cooling air is brought to atmospheric pressure in the event of a station blackout or failure of the suction blowers. To overcome the effect of main blower failure, a series of backup blowers are connected to the vault. Upon failure of the primary mechanical blower, a secondary mechanical blower replaces it. Further, if the secondary mechanical blower fails, the primary diesel generator (DG) supplies power the blower. In case of failure of the primary DG power supply, secondary DG operates the blower. In addition to blower failure, the failure of the chilling plant can lead to a rise in the temperature of cooling air at the inlets. The drying of cooling water at the chilling plant can lead to a rise in the temperature of cooling air at inlets. In a crucial system like a fuel storage vault, it is critical to understand the consequences of numerous mishaps, particularly the loss of cooling air. The temperature should be maintained within the safe limit of 363 K inside the storage vault. Therefore, the objective of the present study is to study and analyze the rise in air temperature and fuels due to complete blackout scenario.

Several studies have been conducted to understand the thermal behavior of various spent and fresh fuel storage vaults under accident scenarios [1]–[4]. The study largely relies on numerical simulations because experimental support and corresponding data generation for accident conditions are difficult to obtain. For example, the accident conditions and safety assessment of the dry nuclear fuel storage facility were analyzed by Alyokhina [2]. The study recommended that, to maintain the safety of the storage facility, heat should be effectively removed from the fuel storage cask. Bixler et al. [3] analyzed the pressure and temperature distributions in an ice condenser plant at a nuclear power generation facility during a short-term station blackout. Wataru et al. [4] performed a heat removal verification test of full-scale concrete cask and concrete-filled steel cask (CFS). They reported that the temperature of air inside the cask remained within safety limits even after 50 % blockage of inlet ducts. Also, the airflow was reduced by 5% and 22% in the concrete and the CFS cask, respectively.

Despite the aforementioned studies on various accident situations in a nuclear fuel storage vault, there are only a very few studies that analyze the transient effect of backup blowers. It is crucial to understand the consequences of various possible mishaps in a sensitive system like a nuclear fuel storage vault, particularly when cooling air is lost. As a result, the primary

goal of this study is to conduct a CFD analysis of a nuclear fuel storage vault after the failure of primary and backup blowers in series. The vertical temperature distributions with respect to time are used to analyze the flow distributions and rise in air temperature in a nuclear fuel storage vault.

2. Numerical analysis

2.1. Computational domain and boundary conditions

The computational domain consists of blanket and fuel enclosures surrounded by a thick concrete wall, as shown in Fig. 1. The components of the vault consist of inlet ducts (ID), blanket subassemblies (BSA) and magazines (BMZ), interconnecting ducts (ICD), fuel subassemblies (FSA) and magazines (FMZ), and outlet ducts (OD). The length of the vault, breadth, and height are 20.72 m, 10.48 m, and 6.67 m, respectively. The thickness of the walls in fuel and blanket enclosure was 0.75 m and 1.5 m, respectively. The subassemblies and magazines are stored in a stainless-steel container of height 4.5 m and diameter 0.282 m and 0.183 m, respectively. A safe distance of 0.57 m is maintained between the containers to prevent them from achieving self-criticality. The blanket enclosure stores 48 BSA and 48 BMZ. The number of FSA and FMZ is stored in the fuel enclosure is 96 each.

The air enters the vault through four L-shaped inlet ducts in a blanket enclosure. The cooling air removes the decay heat from the blankets and enters the fuel enclosure through eight interconnecting ducts where four are placed at the height of 4 m and rest at 1 m from the bottom. The heat is removed from fuels placed in the fuel enclosures and leaves the vault through four S-shaped outlets. The suction pressure is maintained at the outlets to induce air flow and maintain the pressure inside the vault below atmospheric pressure. The sub-atmospheric pressure inside the vault prevents the release of radioactive particles in the surrounding.

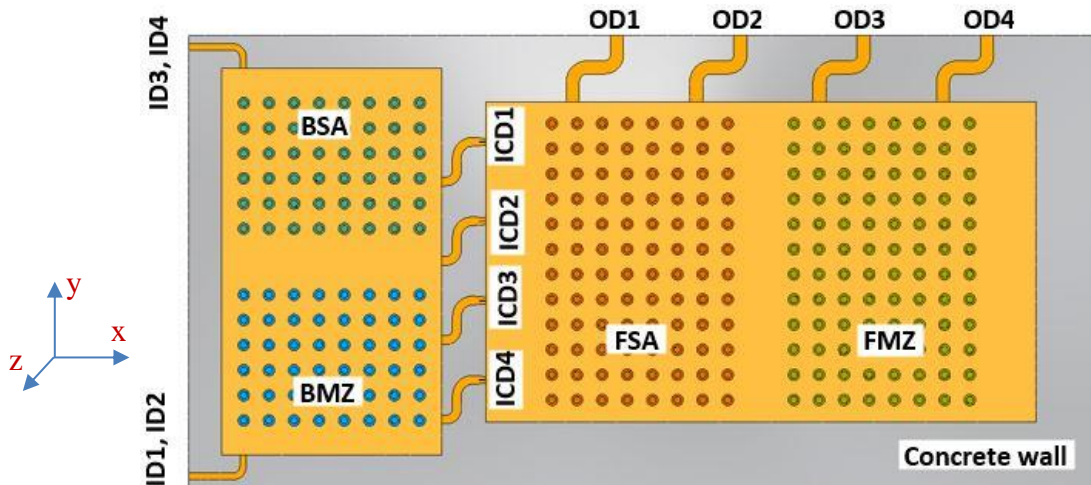


Fig. 1. Schematic plan view of nuclear fuel storage vault.

2.1. Initial and boundary conditions

The transient airflow inside the vault was assumed to be continuous and incompressible. A no-slip boundary condition was applied to the walls, fuels, and blanket containers. The outlet suction pressure (P_o) was dependent on failure and starting of blowers. The heat transfer coefficient through the outer wall of surface area (A) is dependent on the temperature of the wall (T_w) and heat flux (Q) through the walls. The temperature of surrounding air (T_s) was maintained at 300 K initially, which rose to 318 K due to the failure of the chilling plant. The heat generated by the blankets and fuels has been considered as a constant heat flux on the surface of subassemblies and magazines for modelling. The fixed and variable boundary conditions used in the present work are summarized in Tables 1 and 2.

Table 1. Fixed initial and boundary conditions

Sl. No.	Boundaries	No.	Type	Condition
1.	BSA	48	Wall	Heat flux ~1 W
2.	BMZ	48	Wall	Heat flux ~1 W
3.	FSA	96	Wall	Heat flux ~192 W
4.	FMZ	96	Wall	Heat flux ~121 W

Table 2. Variable boundary conditions

Sl. No.	Boundaries	No.	Type	Condition
1.	Inlets	4	Pressure inlet	$t = 0, T_{in} = 300K,$ $t = t_{acc}, T_{in} = 318 K$
2.	Outlets	4	Pressure outlet	$t < 10 s, P_o = -100 Pa$ $15 s < t < 115 s, P_o = 0 Pa$ $120 s < t < 220 s, P_o = -100 Pa$ $225 s < t < 325 s, P_o = 0 Pa$ $330 s < t < 430 s, P_o = -75 Pa$ $435 s < t < 535 s, P_o = 0 Pa$ $540 s < t, P_o = -75 Pa$
3.	Outer wall	96	Wall	$t = 0, T_w = 300 K$ $h = Q / (A \times (T_w - T_s))$

3. Governing equations

The continuity, momentum, and energy equations were solved to simulate the flow field and heat transfer inside the enclosures. In this case, the governing system of equations can be written as follows:

$$\frac{\partial \rho}{\partial t} + \nabla \cdot (\rho \mathbf{u}) = 0 \quad (1)$$

$$\rho \left(\frac{\partial}{\partial t} + \mathbf{u} \cdot \nabla \right) \mathbf{u} = -\nabla P + \rho \mathbf{g} + \nabla \cdot (\mu_{eff} \nabla \mathbf{u}) \quad (2)$$

$$\rho C_p \left(\frac{\partial}{\partial t} + \mathbf{u} \cdot \nabla \right) T = \nabla \cdot (K_{eff} \nabla T) + q''' \quad (3)$$

where, $\rho \mathbf{g}$ is the body forces and q''' is the decay heat generated by blankets and fuels. The equation for Boussinesq approximation is given by

$$(\rho - \rho_o) \mathbf{g} + \rho g \beta (T - T_o) = 0 \quad (4)$$

In equation 4, ρ_o and T_o are the reference density and temperature, respectively. The equations for turbulent kinetic energy and specific rate of dissipation are defined in equations (4) and (5), respectively.

$$\frac{\partial k}{\partial t} + \frac{\partial(\mathbf{u}_j k)}{\partial x_j} = \frac{\partial}{\partial x_j} \left[\left(\nu + \frac{\nu_t}{\sigma_k} \right) \frac{\partial k}{\partial x_j} \right] + \left[\nu_t \left(\frac{\partial(\mathbf{u}_i)}{\partial x_j} + \frac{\partial(\mathbf{u}_j)}{\partial x_i} \right) - \frac{2}{3} k \delta_{ij} \right] \frac{\partial(\mathbf{u}_i)}{\partial x_j} - \varepsilon \quad (5)$$

$$\frac{\partial \varepsilon}{\partial t} + \frac{\partial(\mathbf{u}_j \varepsilon)}{\partial x_j} = \frac{\partial}{\partial x_j} \left[\left(\nu + \frac{\nu_t}{\sigma_\varepsilon} \right) \frac{\partial \varepsilon}{\partial x_j} \right] + C_1 \frac{\varepsilon}{k} \left[\nu_t \left(\frac{\partial(\mathbf{u}_i)}{\partial x_j} + \frac{\partial(\mathbf{u}_j)}{\partial x_i} \right) - \frac{2}{3} k \delta_{ij} \right] \frac{\partial(\mathbf{u}_i)}{\partial x_j} - C_2 \frac{\varepsilon^2}{k} \quad (6)$$

The value of constants is $C_1 = 1.44$; $C_2 = 1.92$; $\sigma_k = 1$; $\sigma_\varepsilon = 1.3$. The turbulent viscosity (μ_t) was calculated using $\mu_t = \rho C_\mu \frac{k^2}{\varepsilon}$, where $C_\mu = 0.09$.

4. Results and discussion

4.1. Grid Independent analysis and validation

The grid independent study was carried out by performing simulations for coarse (5×10^6 cells), medium (10×10^6 cells), and fine (16×10^6 cells) grids (Fig. 2). For this purpose, the meshing was done using the ‘‘ANSYS-Meshing’’ function.

A thorough validation of the present simulated result was carried out (Fig. 3) against the simulated and measured data of Wang and Chen [5], ascertaining the predictive capability of the computational model. The simulated results are in good agreement with the experimental results.

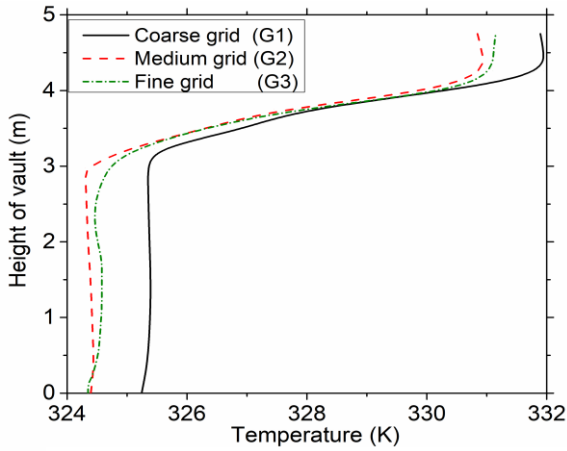


Fig. 2. Analysis of vertical temperature distribution at $x = 9$ m for different grid sizes.

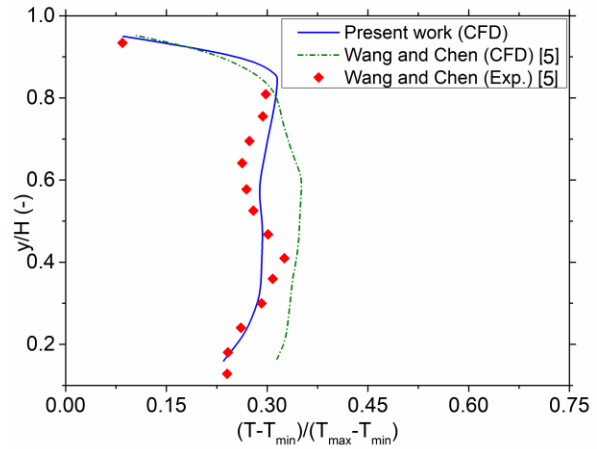


Fig. 3. Comparison of vertical temperature distributions in the enclosure with the predicted and measured data of Wang and Chen [5].

4.2. Temperature distributions

The temperature distributions inside the vault along its length at $y = 5.4$ m, before and after (at $t = 525$ s) the accident is presented in Fig. 4 (a) and (b), respectively. The temperature of the blankets was increased by 11 K, due to a rise in inlet air temperature after failure at the chilling plant. However, the air temperature in the fuel enclosure rose by 15 K due to the combined effect of the rise in inlet air temperature and the stopping of suction blowers. Fig. 5 presents the variation in the average temperature of fuels with time. There was an immediate rise in the temperature of fuels after the failure of blowers. The average temperature of fuels rises to a maximum value of 333 K after the failure of the blowers. The rise in temperature of inlet air and reduction in suction pressure by DG operated blowers were not allowed to bring the average temperature of fuels to normal operating temperature. However, the vault was found to be in safe operating condition even after repeated failure of blowers and rise in temperature of cooling air.

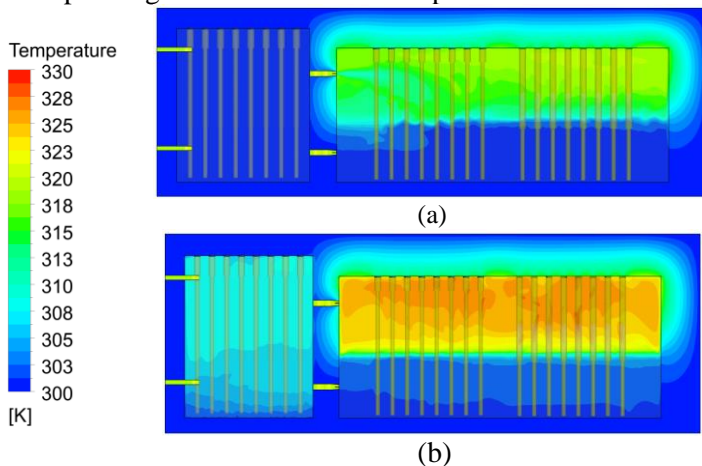


Fig. 4. Temperature distributions inside the vault, (a) before the accident and (b) 525 s after the failure of suction blowers.

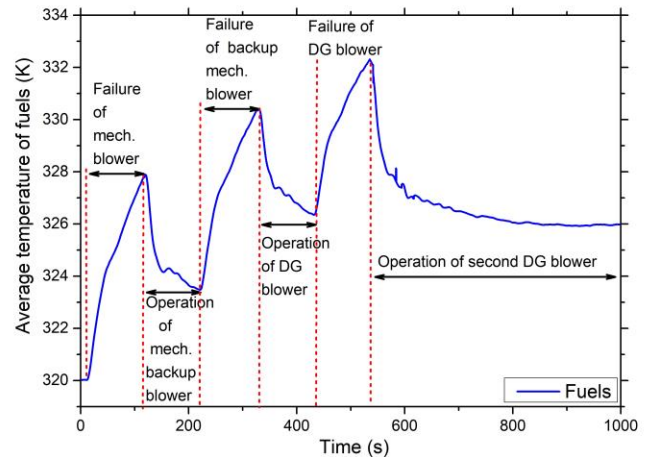


Fig. 5. Variations in the temperature of fuels due to blower failure and operation of backup blowers.

5. Conclusions

In the present work, the rise in air and fuel temperature inside the vault is numerically investigated. In the absence of suction pressure at the outlets, the flow of cooling air was stopped. Three-dimensional simulations of the nuclear fuel

storage vault were carried out to analyze the safety of the vault after repeated failure of the suction blowers. The simulations show that there is an immediate rise in the temperature of fuels in the enclosure. However, with starting of backup blowers, the temperature of fuels was gradually reduced. The temperature of air in blanket enclosures was increased due to a rise in inlet air temperature. In addition, the temperature of fuels did not reach the normal temperature even after starting of suction blowers because of the high temperature of the air entering the vault through the inlets. The present study will be helpful to define accident scenarios based on thermal implications and use the information to develop effective prevention measures for risk mitigation.

Nomenclature

BMZ	Blanket magazine	[-]	T	Temperature	[K]
BSA	Blanket subassemblies	[-]	u	Velocity	[m/s]
FMZ	Fuel magazine	[-]	ρ	Density of air	[kg/m ³]
FSA	Fuel subassemblies	[-]	β	Coefficient of thermal expansion	[1/K]
g	Acceleration due to gravity	[m/s ²]	ε	Specific rate of dissipation	[-]
k	Turbulent kinetic energy	[m ² /s ²]	σ_k	Kinetic energy turbulent Prandtl number	[-]
K_{eff}	Effective thermal conductivity	[W/m-K]	σ_ε	Dissipation rate turbulent Prandtl number	[-]
q'''	Decay heat generated	[W]	μ_t	Turbulent Viscosity	[kg/m-s]

References

- [1] B. Droste, H. Völzke, G. Wieser, and L. Qiao, "Safety Margins of Spent Fuel Transport and Storage Casks Considering Aircraft Crash Impacts," *Int. J. Radioact. Mater. Transp.*, vol. 13, no. 3–4, pp. 313–316, Jan. 2002, doi: 10.1179/rmt.2002.13.3-4.313.
- [2] S. Alyokhina, "Thermal analysis of certain accident conditions of dry spent nuclear fuel storage," *Nucl. Eng. Technol.*, vol. 50, no. 5, pp. 717–723, Jun. 2018, doi: 10.1016/j.net.2018.03.002.
- [3] N. E. Bixler *et al.*, "SOARCA uncertainty analysis of a short-term station blackout accident at the Sequoyah nuclear power plant," *Ann. Nucl. Energy*, vol. 145, p. 107495, Sep. 2020, doi: 10.1016/j.anucene.2020.107495.
- [4] M. Wataru, H. Takeda, K. Shirai, and T. Saegusa, "Heat removal verification tests of full-scale concrete casks under accident conditions," *Nucl. Eng. Des.*, vol. 238, no. 5, pp. 1206–1212, May 2008, doi: 10.1016/j.nucengdes.2007.03.035.
- [5] M. Wang and Q. Chen, "Assessment of Various Turbulence Models for Transitional Flows in an Enclosed Environment (RP-1271)," *HVACR Res.*, vol. 15, no. 6, pp. 1099–1119, Nov. 2009, doi: 10.1080/10789669.2009.10390881.